Lasers in Manufacturing Conference 2021

Improved catalytic activity and surface functionalization of nanoparticles by pulsed laser post-processing of colloids.

Sven Reichenberger[a,b*], Swen Zerebecki[a,b], Stephan Barcikowski[a,b]

[a]*Technical Chemistry I and Center for Nanointegration Duisburg-Essen (CENIDE), University of Duisburg-Essen, 45141 Essen, Germany*
[b]*NanoEnergieTechnikZentrum (NETZ), University of Duisburg-Essen, 47057 Duisburg, Germany*

Abstract

The precise writing of defects and structural alterations into colloidal nanoparticles offers a great application potential. To that end, many studies using pulsed laser post-processing were conducted in the past. Yet, either multi-pulse phenomena and/or intensity gradients linked to the experimental setup rendered gradual and uniform tailoring of material properties complicated. In the presented article a new setup that provides a thin flat liquid jet for continuous laser post-processing of nanoparticles with single laser pulses is presented and discussed. As will be shown, compared to the conventional liquid jet setup with circular cross-section, the new flat jet realizes unprecedented uniformity of laser excitation conditions, significantly decreasing laser intensity deviations. Due to the higher uniformity of the laser treatment, the fragmentation threshold of gold nanoparticles was experimentally evaluated with high resolution and very good agreement with the theoretical prediction. For the conventional liquid jet setup, no threshold was observed. This new uniform laser post-processing of colloidal nanoparticles holds great potential for all applications requiring a tailored design of defect density and materials properties.

Keywords: pulsed laser post-processing of nanoparticles, laser fragmentation, catalysis, metal nanoparticles

1. Introduction

Pulsed laser post-processing (PLPP) of colloidal particles is an important and unique method to prepare surfactant-free nanoclusters, induce phase transitions or alter the defect density, of nanoparticles, while

* Corresponding author.
E-mail address: sven.reichenberger@uni-due.de

operating under high purity and continuous flow conditions (Amendola et al., 2020). Gradually altered materials properties within these laser-processed nanoparticles possess high relevance for studies in applied physics (Z. Lin et al., 2018), material science (Siebeneicher et al., 2020), or catalysis (Waag et al., 2017; Yu et al., 2019) but demand a precise process control. Previous laser processing-based research endeavours were focussing on size-control, structural transformation of realistic mesoporous and nanoparticle functionalized materials, doping, and defect introduction including bandgap engineering in semiconducting thin-film structures or nanoparticles (Amendola et al., 2020). Particularly, laser-induced material strain and surface oxygen vacancies provide large application potentials in heterogenous catalysis e.g. in the development of new energy materials for water splitting (Li et al., 2019; J. Y. Lin et al., 2019). Here, particularly Co_3O_4 spinel has gained much attention since its good activity and stability under alkaline oxygen evolution reaction conditions (Bergmann et al., 2018). For example, sub-5 nm Co_3O_4 nanoparticles from laser fragmentation in liquid (LFL) showed superior activity in a previous study (Yu et al., 2019). Yet, the question remains if the superior activity was linked to the size change, defect formation, or both.

The main driving force for the material alteration is given by the applied laser intensity where the size- and wavelength-dependent absorption cross-section mediates the amount of energy that is absorbed by the nanoparticles (Amendola et al., 2020). Respectively, the nanoparticles will heat up, melt or suddenly evaporate and fragment into smaller pieces. Many fragmentation mechanisms and related intensity ranges were proposed and discussed in the literature (Amendola et al., 2020; Hashimoto et al., 2012) but setup-related multi-pulse phenomena and/or intensity gradients still provide one of the biggest challenges in all these studies. Consequently, the non-uniform laser-processing of the colloidal nanoparticles renders the comparability of the studies complicated and strongly coupled to the used setup. This makes differentiating the catalytic effect of reduced particle size and defect formation during LFL even more complicated when comparing different studies. The liquid jet setup (circular cross-section) using a passage reactor design provided the first step towards better comparability allowing single pulse conditions thereby abandoning previous cross-correlations between laser-induced material changes and the repetition rate. A few years ago, it allowed verifying for the first time that laser fragmentation is a single laser pulse phenomenon (Zerebecki et al., 2020; Ziefuß et al., 2018). Yet, the setup still suffers from intensity gradients induced by the refraction of the laser beam at the gas-liquid interface of the cylindrical liquid jet and a related less uniform colloidal post-processing (Siebeneicher et al., 2020; Waag et al., 2017). In a previous study the phase decomposition, melting, and agglomeration processes observed after PLPP were associated with these intensity gradients and their effect on a laser-induced redox reaction, radical formation, and material defects (Siebeneicher et al., 2020).

Here we present a newly developed and recently discussed flat jet setup (Zerebecki et al., 2020) that allowed to significantly reduce intensity gradients, single pulse particle processing, and uniform illumination of all particles in a continuously operating flow. The calculated intensity profiles and intensity deviations of a laser pulse with standardized Gaussian and top-hat intensity profiles in the old and new setup will be compared and discussed in the frame of the fragmentation threshold found for colloidal gold nanoparticles as reference materials.

2. Materials and methods

The PLPP experiments were conducted in a self-build flat jet setup shown in Fig. 1 a) and in line with a previous publication (Zerebecki et al., 2020). In the setup, a colloid is circulated from a reservoir and pumped through a 250 µm slit nozzle to form a flat liquid jet of 130 µm thickness (Zerebecki et al., 2020). Individual laser pulses emitted by an Nd:YAG laser (IS400-1-L, SHG, Edgewave) are applied in the center of the flat jet with a pulse duration of 7 ns, a wavelength of 532 nm, and maximal pulse energy of 10 mJ at 5 kHz repetition rate. The laser-treated central section of the flat jet is cut out with the help of two self-made Teflon knives

which are 1 mm apart. To ensure full illumination of this separated volume element the distance was chosen in line with the width of the laser beam. By tuning the mean residence time of each colloid-containing volume element in the cut-out section to match the temporal inter pulse distance of the laser, single pulse per volume element conditions are maintained. Further experimental details are reported in (Zerebecki et al., 2020).

To compare the flat jet setup with the conventional liquid jet of circular cross-section using standardized laser intensity profiles conditions, ray tracing calculations were conducted assuming a perfect gaussian (according to ISO13694:2000) and top hat intensity profile of the laser, a 45 nm gold colloid, and a concentration of 1 g/L. The calculations are in line with a previous study where a realistic intensity profile was used as the basis for a similar calculation (Zerebecki et al., 2020). Laser fragmentation experiments were performed with colloidal 45 nm gold nanoparticles as educt previously prepared by a Turkevich synthesis (Zerebecki et al., 2020). The educt nanoparticle colloid was illuminated with single laser pulses of different laser intensity with fluences above 1 J/cm^2 (Fig. 1b).

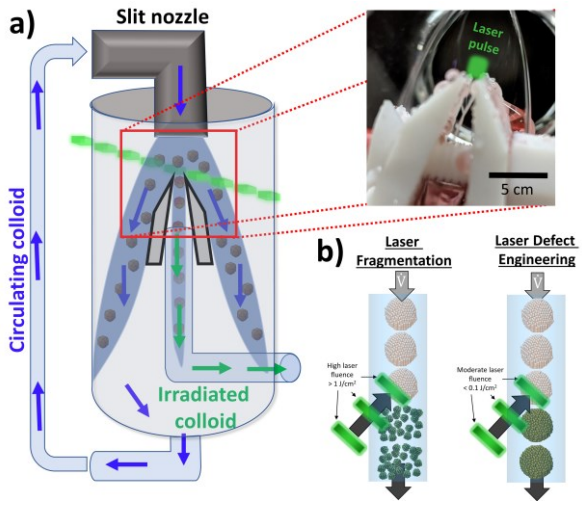

Fig. 1. a) Illustration of the flat jet setup for uniform laser post-processing of colloids; b) conceptional comparison of laser fragmentation and laser defect engineering in liquids

3. Results and discussion

Fig. 2 a) depicts the calculated intensity profile of a Gaussian beam when passing through the conventional liquid jet with a circular cross-section. In line with previous results (Siebeneicher et al., 2020; Waag et al., 2017), the laser is refracted at the gas-liquid phase boundary of the spherical liquid jet cross-section, leading to focusing in the central part and non-irradiated sections in the right upper and lower part of the cross-section. Additionally, the beam is significantly attenuated by the absorption and scattering at the present nanoparticles present in the liquid jet. For the new flat jet setup shown in Fig. 2 b) no refraction occurs while the attenuation is significantly reduced due to the much shorter liquid layer thickness. Consequently, a higher uniformity of the intensity profile in the whole irradiated liquid cross-section is achieved. In Fig. 2 c) the intensity deviation, gained from averaging the intensity profile of each setup over the whole liquid cross-section is presented (for irradiating a 45 nm-sized gold colloid and 1 g/L concentration with 532 nm laser pulses). The intensity deviation, which is equivalent to the intensity error bar in such an experiment reaches nearly 100 % in the conventional setup (red bars). The only 48% smaller deviation of the Gaussian beam in the flat jet setup yet puts this high value somewhat into perspective (blue bars). Obviously, about 50% of the deviation in the conventional liquid jet setup was still caused by the intensity deviation of the gaussian beam

itself. From the calculated deviation for the top-hat laser beam in the flat jet, it is also evident, that about 15% of attenuation was also caused by interactions (extinction) with the nanoparticles at a given concentration, wavelength, size, and material system. Overall, it is evident, that the new flat jet setup reduces the intensity deviation significantly, allowing a more uniform single laser pulse post-processing.

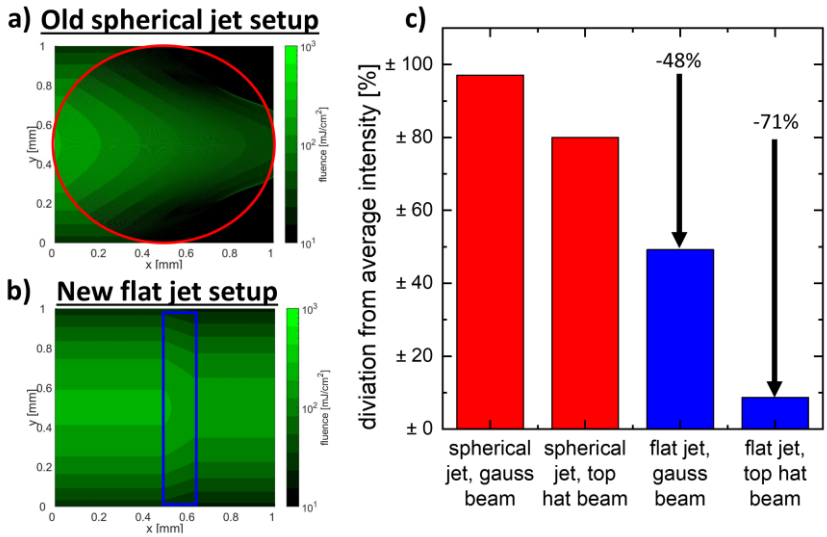

Fig. 2. Simulated intensity profile of a Gaussian beam passing through a) the old circular-shaped liquid jet; b) the new flat jet setup. c) Calculated intensity deviation of a laser beam when passing through the old (Ziefuß et al., 2018) and new (Zerebecki et al., 2020) setup assuming a gaussian and a top hat laser beam intensity profile.

The previous statement was tested by performing laser fragmentation of a 45 nm gold colloid (Fig. 3 a) at different laser intensities. The theoretically expected fragmentation intensity threshold of these gold colloids was previously calculated (Zerebecki et al., 2020). As depicted in Fig 3 b) a significant reduction of the surface plasmon resonance (caused by a size reduction) can be observed over a small laser intensity range in the case of LFL experiments using the flat jet setup (shown in blue), which agrees well with the theoretically expected fragmentation regime of the 45 nm gold nanoparticles. In turn, the results found in the cylindrical setup are smeared out due to the high-intensity deviation, such that fragmentation was already observable at average laser intensity that was significantly smaller than the expected fragmentation regime. In conclusion, the flat jet setup allows more uniform laser post-processing of colloids when sufficient laser power is available while the liquid jet on the other hand also allows fragmentation even with less intense lasers. Hence, both setups bear their advantages depending on the experimental question.

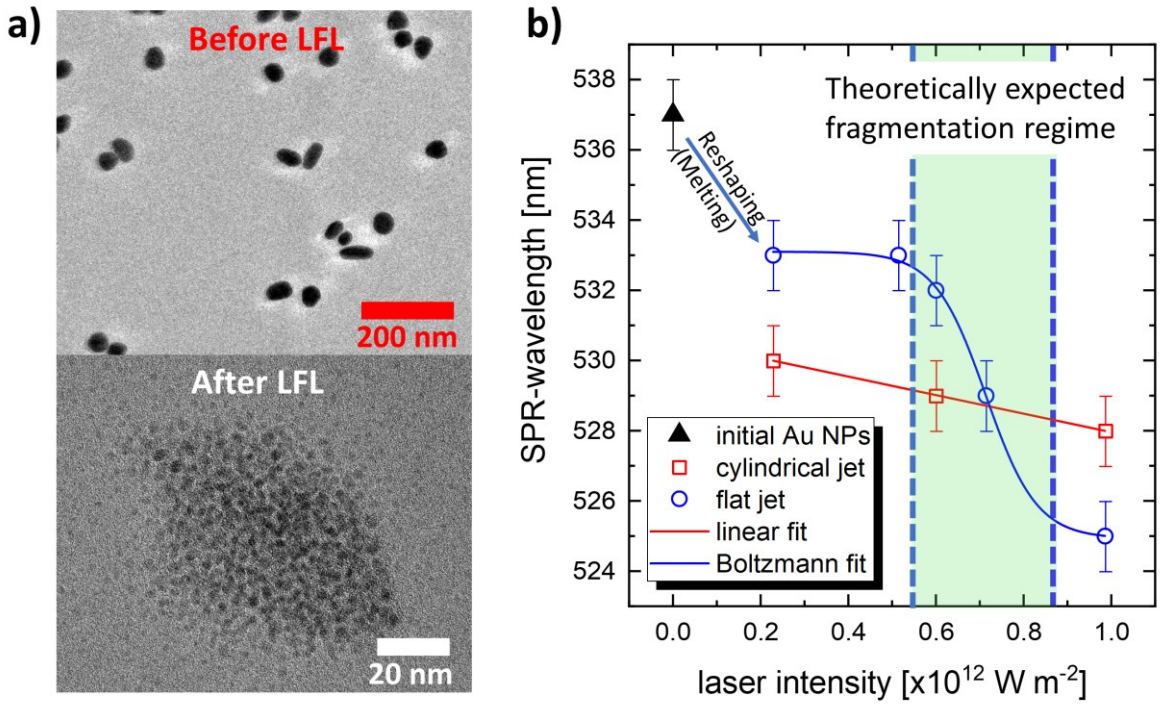

Fig. 3. a) TEM images of gold nanoparticles before and after laser fragmentation (LFL); b) measured SPR shift of colloidal gold nanoparticles after LFL was performed with different laser intensities within the old circular and new flat jet setup.

4. Conclusion

The recently developed flat jet setup allows laser post-processing of colloidal nanoparticles with single laser pulses, uniform illumination, and minimized laser intensity gradients under continuous flow conditions. In conventional liquid jet setups with a circular cross-section, the intensity gradients can reach up to 100 % of the average value for a gaussian laser beam profile. For the new flat jet setup, this attenuation was reduced to about 50%, which is mainly caused by the intensity variation from the gaussian intensity profile. In the case of a gradient-free top-hat beam profile, the attenuation was reduced from 80% (conventional liquid jet) down to only 15% (new flat jet setup), with the latter being solely due to the beam attenuation. Note, that the 15% already represents a worst-case estimation since the colloid concentration was intentionally chosen very high (1 g/L) compared to the laser post-processing studies of colloids normally reported (<< 0.1 g/L, Amendola et al., 2020). The improved intensity-uniformity was put to a practical evaluation in a fragmentation experiment with gold nanoparticles as reference materials. The observed fragmentation threshold was in very good agreement with theoretical predictions. On the other hand, for the conventional liquid jet setup, no clear fragmentation threshold could be observed. Yet, due to the high-intensity gradients of up to 100%, fragmentation was achieved even when the laser intensity was much lower than the expected threshold, rendering this setup especially valuable for experiments with low-powered laser setups. Consequently, the presented continuously operating flat jet setup represents a novel laser post-processing technique for uniform laser-based defect engineering of colloidal nanoparticles highly relevant but not limited to catalytic studies.

Acknowledgments

We gratefully acknowledge the DFG Deutsche Forschungsgemeinschaft for its financial support under the Project 388390466 – TRR 247. Dr. Marcus Heidelmann (ICAN) is acknowledged for assistance with HRTEM measurements.

References

Amendola, V., Amans, D., Ishikawa, Y., Koshizaki, N., Scirè, S., Compagnini, G., Reichenberger, S., & Barcikowski, S. (2020). Room-Temperature Laser Synthesis in Liquid of Oxide, Metal-Oxide Core-Shells, and Doped Oxide Nanoparticles. *Chemistry – A European Journal*, *26*(42), 9206–9242. https://doi.org/10.1002/chem.202000686

Bergmann, A., Jones, T. E., Martinez Moreno, E., Teschner, D., Chernev, P., Gliech, M., Reier, T., Dau, H., & Strasser, P. (2018). Unified structural motifs of the catalytically active state of Co(oxyhydr)oxides during the electrochemical oxygen evolution reaction. *Nature Catalysis*, *1*(9), 711–719. https://doi.org/10.1038/s41929-018-0141-2

Hashimoto, S., Werner, D., & Uwada, T. (2012). Studies on the interaction of pulsed lasers with plasmonic gold nanoparticles toward light manipulation, heat management, and nanofabrication. *Journal of Photochemistry and Photobiology C: Photochemistry Reviews*, *13*(1), 28–54. https://doi.org/10.1016/j.jphotochemrev.2012.01.001

Li, Z., Zhang, Y., Feng, Y., Cheng, C. Q., Qiu, K. W., Dong, C. K., Liu, H., & Du, X. W. (2019). Co3O4 Nanoparticles with Ultrasmall Size and Abundant Oxygen Vacancies for Boosting Oxygen Involved Reactions. *Advanced Functional Materials*, *29*(36), 1–9. https://doi.org/10.1002/adfm.201903444

Lin, J. Y., Xi, C., Li, Z., Feng, Y., Wu, D. Y., Dong, C. K., Yao, P., Liu, H., & Du, X. W. (2019). Lattice-strained palladium nanoparticles as active catalysts for the oxygen reduction reaction. *Chemical Communications*, *55*(21), 3121–3123. https://doi.org/10.1039/c9cc00447e

Lin, Z., Du, C., Yan, B., Wang, C., & Yang, G. (2018). Two-dimensional amorphous NiO as a plasmonic photocatalyst for solar H 2 evolution. *Nature Communications*, *9*(1), 1–11. https://doi.org/10.1038/s41467-018-06456-y

Siebeneicher, S., Waag, F., Escobar Castillo, M., Shvartsman, V. V., Lupascu, D. C., & Gökce, B. (2020). Laser Fragmentation Synthesis of Colloidal Bismuth Ferrite Particles. *Nanomaterials*, *10*(2), 359. https://doi.org/10.3390/nano10020359

Waag, F., Gökce, B., Kalapu, C., Bendt, G., Salamon, S., Landers, J., Hagemann, U., Heidelmann, M., Schulz, S., Wende, H., Hartmann, N., Behrens, M., & Barcikowski, S. (2017). Adjusting the catalytic properties of cobalt ferrite nanoparticles by pulsed laser fragmentation in water with defined energy dose. *Scientific Reports*, *7*(1), 1–13. https://doi.org/10.1038/s41598-017-13333-zf

Yu, M., Waag, F., Chan, C. K., Weidenthaler, C., Barcikowski, S., & Tüysüz, H. (2019). Laser Fragmentation-Induced Defect-Rich Cobalt Oxide Nanoparticles for Electrochemical Oxygen Evolution Reaction. *ChemSusChem*, *13*(3), 1–10. https://doi.org/10.1002/cssc.201903186

Zerebecki, S., Reichenberger, S., & Barcikowski, S. (2020). *Continuous-Flow Flat Jet Setup for Uniform Pulsed Laser Postprocessing of Colloids*. https://doi.org/10.1021/acs.jpca.0c08787

Ziefuß, A. R., Reichenberger, S., Rehbock, C., Chakraborty, I., Gharib, M., Parak, W. J., & Barcikowski, S. (2018). Laser Fragmentation of Colloidal Gold Nanoparticles with High-Intensity Nanosecond Pulses is Driven by a Single-Step Fragmentation Mechanism with a Defined Educt Particle-Size Threshold [Research-article]. *Journal of Physical Chemistry C*, *122*(38), 22125–22136. https://doi.org/10.1021/acs.jpcc.8b04374